A Study of Heat Input Distribution on the Surface during Torch Weaving in Gas Metal Arc Welding

Y. Kim and H. Park

Abstract

In weaving welding where a V groove exists, the heat input distribution is an important factor that determines the defectiveness of the bead shape, undercut and over-lap. In this study, the amount of heat input, which is determined by the welding current, voltage, speed and weaving conditions is calculated through mathematical development and numerical methods. Furthermore, the heat input distribution as a two- dimensional heat source was observed when applied to each groove.

Key Words : Torch weaving, Arc welding, Gaussian distribution, Heat input distribution, Undercut.

Nomenclature

B_r	wire burning rate
F_r	wire feed rate
f	weaving frequency
H	inductance
I	mean welding current
k	distribution coefficient
L	contact tube to workpiece distance (CTWD)
L_a	arc length
L_x	length of the wire extension
O_1	operating point
O_2	new operating point
Q	heat input per unit time
$q(r)$	heat flux per unit area per unit time deposited at location
R	circuit resistanceecause
R_h	heat input radius
r	distance from the center of the arc
V	mean welding voltage
V_{input}	welding input voltage
V_{ref}	reference welding voltage
V_{oc}	open circuit voltage
v_g	torch speed on the groove surface
v_x	torch speed of xaxis direction
v_y	torch speed of yaxis direction
v_z	torch speed of zaxis direction
v_w	welding speed
W	weaving width
z	groove height
η	arc efficiency
λ	welding voltage control width coefficient
θ	groove angle
$a, b, K_0, K_1, K_2, m, p, s, V_0, \alpha, \beta$	coefficients

Y. Kim : Welding Technology Research Team, Doosan Heavy Industries & Construction Co., Ltd., Changwon, Korea
E-mail : yongjaekim@doosanheavy.com
H. Park : Manufacturing Engineering R&D Team, KIA Motors, Kyungki, Korea
E-mail : hpark21@kia.co.kr

1. Introduction

Gas metal arc welding (GMAW), the process that melts the continually supplied wire and base metal by generating an electrical arc between them, is the most widely used welding method because of its flexibility for automation and in-process applicability. The arc is

in a high temperature, acts as a passageway from the molten drop to the base metal. Also, the arc directly applies heat input to the base metal surface, greatly affecting the temperature distribution of the base metal. Such temperature distribution is important factor in determining weld quality such as weld pool shape, size of heat affected zone, and chemical formation of the weld part. Therefore, despite the complexity and non-linearity of the welding process, it becomes necessary to study the analytic prediction of the temperature distribution of the workpiece with the arc phenomenon.

In his research, Rosenthal[1] presented the first analytical model, by explaining the heat conduction at the quasi-stationary state, with a point or line heat source. However, his idealistic model that included many assumptions showed large error in estimating actual temperature distribution. The development of computer technology in the 1980s made it possible to expeditiously perform complex calculation, and as analysis through finite element method and finite difference method were enabled, active research was performed to reduce errors of the existing models. Through a research which expanded the stationary heat source to an moving heat source, Eagar and Tsai[2] attempted to explain 2 and 3-dimensional temperature distribution in gas tungsten arc welding (GTAW). Later studies used moving heat sources with Gaussian distribution as heat sources. Tsao and Wu [3] presented a 2-dimensional heat transfer model in GMAW, while Tekriwal and Mazumder [4] suggested a 3-dimensional model. Later, Kim and Na[5] were able to make more accurate temperature distribution estimations through 3-dimensional temperature distribution explanations using boundary-fitted coordinates. The above studies are all explanations of bead on plate welding. Recently, Jeong and Cho[6] used the mapping method to explain 3-dimensional temperature distribution in fillet welding, while Moon and Na[7] performed studies to understand the temperature distribution estimation of fillet welding, and the cause of defect generation. However, a detailed explanation of heat input variance in weaving welding, which is the generally used method for fillet welding has not yet investigated.

Weaving the torch was performed to cover the seam zone with deposited metal as well as to use the arc sensor. In this case, the welding current and voltage were changed according to the weaving location, not only causing the entire heat input amount to change, but also altering the heat input distribution which appears on the groove surface. Although the mathematical explanation of such phenomenon is necessary to understand the generation mechanism of the overlap and undercut that occur during weaving while estimating the weld pool formation and bead formation, only an experimental approach has been taken, due to the complexity of the process. Moon[8] suggested a method of determining the offset by comparing the current variation patterns ensuing the generation of undercut or overlap, and Kim and Rhee [9] researched into the prevention of heat input concentration at the weaving end by controlling the wire feed rate. However, the extent to which seam tracking and weld quality enhancement can be performed under possibility of undercut generation was limited, and it is very difficult for the wire feed rate to be controlled, sine the wire is curved and slipped between the rollers. Especially the wire feed rate cannot be measured accurately.

Therefore, in this study, an explanatory observation of the heat input distribution on the groove surface was made, to understand the weld pool formation process according to the heat input distribution while weaving the torch for fillet welding. This was set as a basis of the heat input control, in order to obtain better welding quality. To do this, the weaving conditions and ensuing welding current and voltage variation was explained through the mathematical developments and numerical methods. The heat input distribution was explained through the application to various forms of grooves, and the results were observed.

2. Mathematical modeling of the welding current and voltage

The welding current and voltage that determine the heat input were shown in equations regarding the weaving conditions and the various patterns were

observed through the numerical methods.

In the welding process, the change in arc length was the most important factor in determining the welding current. The arc length was determined through the arc characteristic equation (1), power source characteristic equation (2), and arc maintenance equation (3).

$$V = V_0 + aI + \beta L_a \tag{1}$$

$$V = V_{oc} - RI - H\frac{dI}{dt} \tag{2}$$

$$\frac{dL_x}{dt} = F_r - B_r \tag{3}$$

Where, V is the mean welding voltage, I is the mean welding current, L_a is the arc length, V_{oc} is the open circuit voltage, R is the circuit resistance, H is the inductance, L_x is the length of the wire extension, B_r is the wire burning rate, F_r is the wire feed rate, V_0 and , α, β are coefficients.

If the wire melting characteristic equation (4) and wire extension equation (5) are added to this equation, the welding current value is obtained as equation (6).[10]

$$B_r = aI + bL_xI^2 \tag{4}$$

$$L_x = L - L_a \tag{5}$$

$$\begin{aligned} &K_0\frac{d^2I}{dt^2} + (bK_0I^2 - K_1)\frac{dI}{dt} \\ &+ aI + b(L - K_2 - K_1I)I^2 \\ &= F_r - \frac{dL}{dt} \end{aligned} \tag{6}$$

$$K_0 = \frac{H}{\beta},\ K_1 = -\frac{R+\alpha}{\beta},\ K_2 = \frac{V_{oc} - V_0}{\beta}$$

Where, L is the contact tube to workpiece distance (CTWD), and a, b, K_0, K_1 and are coefficients.

The values used here for calculation are V = 15.7V [11], α = 1/45V/A[12], β = 0.7V/mm[12], V_{oc} = 26.53V[11], R = 1/42 Ω[11], a = 0.33mmA^{-1}s^{-1} [13], b = 0.00005A^{-2}s^{-1} [13], H = 0.00016Henrry[11]. The change in current becomes the function of the CTWD and wire feed rate. When the wire feed rate is constant, the current is determined by the CTWD and CTWD variance rate.

The x axis is the weaving direction, the y axis is the welding direction and the z axis is the vertical direction. The torch weaves over the flat V groove with a groove angle of θ at a welding speed of v_w mm/sec, weaving width of Wmm, and weaving frequency of f *Hz*. Hence, the location and speed of the welding torch at each direction are as shown in equations (7)~(12).

$$x = \frac{W}{2}\sin 2\pi ft \tag{7}$$

$$v_x = \frac{dx}{dt} = W\pi f\cos 2\pi ft \tag{8}$$

$$y = v_w t \tag{9}$$

$$v_y = \frac{dy}{dt} = v_w \tag{10}$$

$$z = |x\cdot\cot\frac{\theta}{2}| = \frac{W}{2}\cot\frac{\theta}{2}\cdot|\sin 2\pi ft| \tag{11}$$

$$v_z = \frac{dz}{dt} = \begin{cases} W\pi f\cot\frac{\theta}{2}\cdot\cos 2\pi ft & \left(0 \le t \le \frac{0.5}{f}\right) \\ -W\pi f\cot\frac{\theta}{2}\cdot\cos 2\pi ft & \left(\frac{0.5}{f} \le t \le \frac{1}{f}\right) \end{cases} \tag{12}$$

Thus, the torch speed on the groove surface, v_g, can be expressed as in equation (13).

$$\begin{aligned} v_g &= \sqrt{(\frac{dx}{dt})^2 + (\frac{dy}{dt})^2 + (\frac{dz}{dt})^2} \\ &= \sqrt{W^2\pi^2\cos^2(2\pi ft)\csc^2\frac{\theta}{2}v_w^2} \end{aligned} \tag{13}$$

For V groove, a weld pool depression is produced at the end of the weave because of the relatively large arc force and electromagnetic force. At the center of the weave, a weld metal deposit is accumulated from molten metal dripping from each of the groove sides. Therefore, the groove form can be assumed as U type rather than V type while welding is performed.

The form of the groove cross section during welding is assumed as equation (14) when welding conditions are as follows : weaving width of 8mm,

groove angle of 90°.

$$z = s(x-m)^4 + p \quad (14)$$

Where, z is the groove height, s is approximately 0.0038, m is 0, and p is approximately 2.06mm. Here, we assumed that the weld pool width is larger than the weaving width and the cross section area of the U groove is the same as that of V groove.

If the height of the groove according to weaving location in equations (14) and (7) are transferred to values according to time, they are as shown in equations (15) and (16).

$$z = s(\frac{W}{2}\sin 2\pi ft - m) + p \quad (15)$$

$$v_z = \frac{dz}{dt} = 4sW\pi f \cdot \cos 2\pi ft(\frac{W}{2}\sin 2\pi ft - m)^3 \quad (16)$$

If we assume the CTWD at the seam for V groove is L_v=20mm , the CTWD for modified U groove is $L=20 - z$. When equations (15) and (16) are substituted into this equation, the following equations (17) and (18) are obtained.

$$L = 20 - s(\frac{W}{2}\sin 2\pi ft - m)^4 - p \quad (17)$$

$$\frac{dL}{dt} = -4sW\pi f\cos 2\pi ft(\frac{W}{2}\sin 2\pi ft - m)^3 \quad (18)$$

If the welding speed of equations (17) and (18) is set at 4mm/sec, the weaving width at 8mm, weaving frequency at 1Hz, and the wire feed rate at 5.5m/min, the non-linear differential equation can be solved through the numerical method. Fig. 1 shows the variation of the welding current and arc length according to time.

It was observed that the welding current gradually increased as the torch approached the side of the groove, and suddenly decreased as it moved further from the side of the groove. This was because when the torch approached the side of the groove, the melting rate increased with the current because of the decrease in CTWD, but the melting rate could not catch up with the weaving speed, causing the current to increase even more. On the other hand, when the torch approached the center, the speed of electrode extension increased due to the decrease in wire melting rate was slower than the weaving speed, causing a larger drop in current. Therefore, through methods such as comparing the left and right integrated welding current during a quarter cycle of weaving, the seam that the torch has deviated from was detected, and the arc sensor which can track the seam was applied[11].

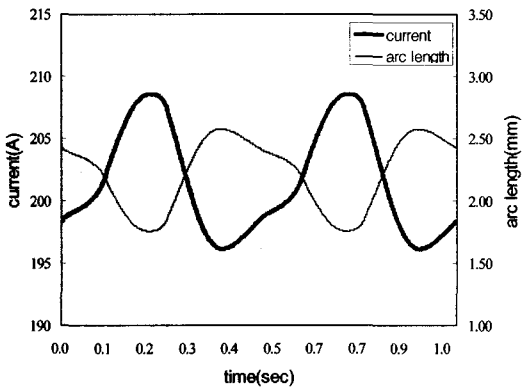

Fig. 1 Current and arc length variation with time

It was observed that the arc length was not constant throughout weaving, but was shortest near the weaving end, and longest near the seam. This meant that the arc radius at the surface of workpiece became smaller at the weaving end. Also, the welding voltage followed the same pattern of variance as the arc length, and changed during weaving according to the length of the arc. However, because of the power source characteristics of the constant voltage mode, the range of variance was very small compared to the change in current, maintaining an almost constant value.

3. Surface heat input distribution

In order to observe the heat input distribution of the groove surface considering the welding current, arc

length, welding voltage and welding speed calculated in the previous section, the heat source was assumed to be 2-dimensional, and a computer simulation was performed of weaving on a flat surface, V groove, and U groove.

3.1 Gaussian distribution

Because the actual heat source is not a point, the 2-dimensional Gaussian distribution was adopted as the heat source. Equation (19)[4] shows the heat input distribution equation in which the heat input radius expands through 99% of the distribution, and the heat input radius during welding was assumed to have a linear proportional relationship with the arc length (heat input radius, $R_h=0.4L_a$).[14]

$$q(r)=\eta\frac{Q}{k\pi R_k^2}\exp(-\frac{r^2}{kR_k^2}) \qquad (19)$$

Where, $q(r)$ is the heat flux per unit area per unit time deposited at location r, η =0.75 is the arc efficiency, $Q = VI$ is the heat input per unit time, k=1/4.6 is the distribution coefficient, $r=\sqrt{x^2+y^2}$ is the distance from the center of the arc and R_h is the heat input radius.

3.2 The heat input distribution on the groove

3.2.1 Flat surface

First, the arc length and shape when weaving on a flat surface were obtained. The results are shown in Fig. 2. The arc length maintained a constant value of 2.64mm, and the welding current and voltage also remained constant. Fig. 3 shows the heat input distribution on the groove of this case. The arc length remained constant, but because the welding speed at the weaving end was slow, the heat input was concentrated on this area. Here, the heat input per unit area had a maximum value of 557.4Joule/mm^2 and a mean value of 33.42 Joule/mm^2. Therefore, it could be seen that when the welding current and voltage remained constant, the welding speed on the groove greatly effected the heat input distribution on a flat surface.

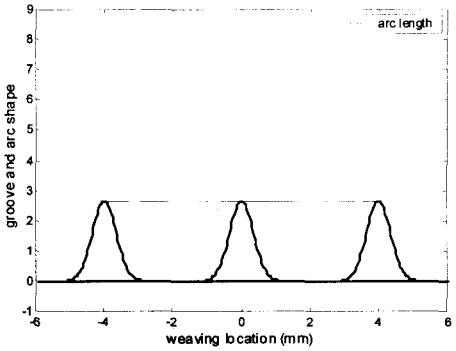

Fig. 2 Groove and arc shape on flat plate

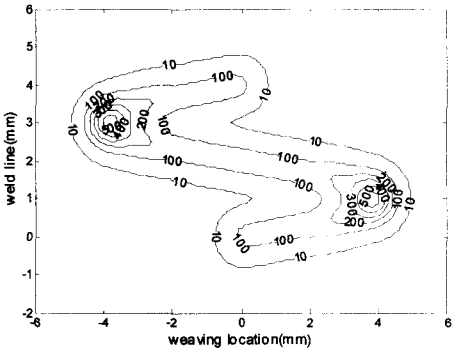

Fig. 3 Heat input distribution on flat plate

3.2.2 V groove

Fig. 4 shows the arc length and shape when weaving on a V groove. The arc length was observed as 4.11mm at the weaving center, and 1.32mm at the weaving end. The heat input distribution is shown in Fig. 5. Here, the maximum heat input value was 1105 Joule/mm^2, while the mean value was 24.16 Joule/mm^2. The heat input showed a higher value when the torch approached the weaving end, than when it approached the weaving center. This was because, as mentioned in the interpretation of current variance according to the weaving location in section 2.1, the weaving speed variation was always larger than the arc length variance according to the CTWD variance, or the melting rate variation according to the current variation. Thus, when the torch approached the weaving end, the current increased, which caused an increase in the heat input, and when the torch

approached the weaving center, the current dropped drastically, causing the heat input to decrease. Of course, in the latter, the increase in arc voltage due to the lengthening of the arc does caused an increase in heat input, but the heat input decreased due to the drop in current has a much stronger effect, resulting in a decrease in the heat input per unit area.

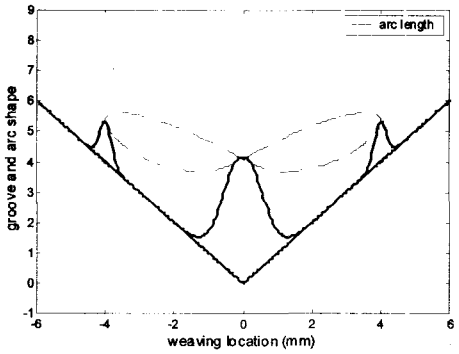

Fig. 4 Groove and arc shape on V groove

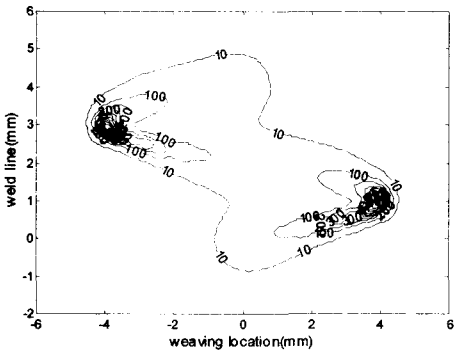

Fig. 5 Heat input distribution on V groove

Also, the arc length was short at the weaving end, and the arc area is relatively small at the surface of the workpiece, resulting in a comparatively larger heat input than at the weaving center. Therefore, the melting more progressed at the weaving end, forming a U shaped groove.

3.2.3 U groove

Fig. 6 shows the arc length and shape of the U groove, which was formed in actual welding. The shape of the U groove was assumed through equation (14). The arc length was 2.44mm at the weaving center, and 1.81mm at the weaving end. Fig. 7 shows the heat input distribution. At the weaving end, the area, which comes into contact with the arc, was larger than that of the V groove, causing a smaller heat input. However, it could be seen that the heat input remains concentrated at the weaving end. The maximum heat input value was 460.5Joule/mm^2, while the mean value was 25.93Joule/mm^2.

The concentration of the heat input at the weaving end was stronger when the groove angle was smaller, and weaving width was wider. This not only limits the weaving width in actual welding, but also caused weld defects in the undercut due to the tracking error when the arc sensor was implemented. Therefore, future research into the control of heat input was necessary.

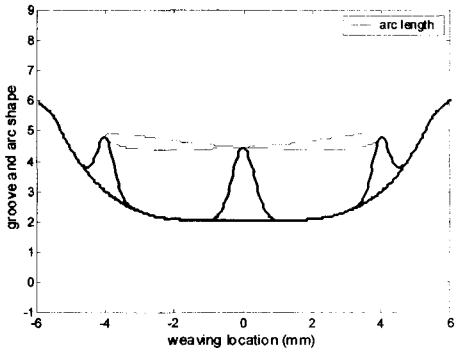

Fig. 6 Groove and arc shape on U groove

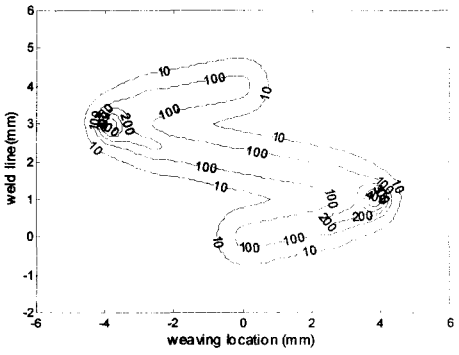

Fig. 7 Heat input distribution on U groove

4. Conclusion

Through an equation which considered welding power source, open circuit voltage, the melting rate of

the electrode and the wire feed rate, a nonlinear differential equation which expressed the welding current variation according to the CTWD and CTWD variation rate was induced. The weaving speed on the groove surface and the weaving trajectory were substituted into the equation to observe the welding current variation, arc length variation and welding voltage variation during the weaving on the U groove. As a result, the welding current increased when the torch approached the weaving end, and decreased drastically when the torch approached the weaving center. And it was observed that the arc length was not constant throughout weaving, but was shortest near the weaving end, and longest near the seam. It was also confirmed that the arc voltage changes in proportion to the arc length. Based on the above results, the heat input which was determined by the welding current and voltage were calculated, to observe the heat input distribution of the groove surface. This was assumed as a heat source which has a 2-dimensional Gaussian distribution, and was applied to a flat surface, V groove and U groove to observe the heat input distribution contour, mean heat input value and maximum heat input value.

References

1. D. Rosenthal : Mathematical theory of heat distribution during welding and cutting, *Welding Journal*, Vol. 20, No. 5 (1941), pp. 220s-234s
2. T. W. Eagar and N. S. Tsai : Temperature fields produced by traveling distributed heat sources, *Welding Journal*, Vol. 62, No. 12 (1983), pp. 346s-355s
3. K. C. Tsao and C. S. Wu : Fluid flow and heat transfer in GMA weld pools, *Welding Journal*, Vol. 67, No. 3 (1988), pp. 70s-75s
4. P. Tekriwal and J. Mazumder : Finite element analysis of three-dimensional transient heat transfer in GMA welding, *Welding Journal*, Vol. 67, No. 7 (1988), pp. 150s-156s
5. J. W. Kim and S. J. Na : A study on the three-dimensional analysis of heat and fluid flow in gas metal arc welding using boundary-fitted coordinate, *Transactions of the ASME*, Vol. 116, No. 2 (1994), pp. 78-85
6. S. K. Jeong and H. S. Cho : An analytical solution to predict the transient temperature distribution in fillet arc welds, *Welding Journal*, Vol. 76, No. 6 (1997), pp. 223s-232s
7. H. S. Moon and S. J. Na : A study on mathematical modeling and heat transfer analysis to predict weld bead geometry in horizontal fillet welding, *Journal of The Korean Welding Society*, Vol. 14, No. 6 (1996), pp. 58-67
8. H. S. Moon : A study on selection of adequate welding parameter by considering weld bead shape and weld defects and development of seam tracker in horizontal fillet welding, Ph. D. Thesis, *Korea Advanced Institute of Science and Technology*, (1996)
9. Y. Kim and S. Rhee : A study of arc sensor considering weaving speed and wire feed rate, *Proceedings of the 1997 fall annual meeting of korean welding society*, (1997), pp. 253-256
10. E. Murakami, K. Kugai, and H. Yamanoto : Dynamic analysis of arc length and its application to arc sensing, *Sensors and Control Systems in Arc Welding*, (1994), pp. 216-226
11. Y. Kim and S. Rhee : Development of arc sensor model using fuzzy controller in gas metal arc welding, *Measurement Science and Technology*, Vol. 12, No. 4 (2001), pp. 534-541
12. M. E. Shepard and G. E. Cook : A nonlinear time-domain simulation of self-regulation in gas-metal arc welding, International Trends in Welding Science and Technology, *Proceedings of the 3rd International Conference on Trends in Welding Research*, (1993), pp. 905-910
13. J. Norrish : Advanced welding processes, *Institute of Physics Pub*, (1992), pp. 147
14. J. F. Lancaster : The physics of welding, *Pergamon Press*, (1984)